ZIBELINE INTERNATIONAL PUBLISHING

ISSN: 2590-4043 (Online)
CODEN: AEMCDV

Acta Informatica Malaysia (AIM)

DOI: http://doi.org/10.26480/aim.01.2023.01.07

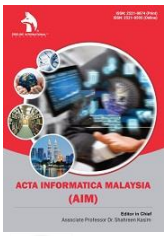

RESEARCH ARTICLE

TRANSFER LEARNING MODELS COMPARISON FOR DETECTING AND DIAGNOSING SKIN CANCER

Peshraw Ahmed Abdalla[a]*, Abdalbasit Mohammed Qadir[b], Omed Jamal Rashid[a], Sarkhel H. Taher Karim[a], Bashdar Abdalrahman Mohammed[a], Karzan Jaza Ghafoor[a]

[a]Computer Science Department, College of Science, University of Halabja, Halabja 46018, Kurdistan Region, Iraq
[b]Computer Science Department, College of Science and Technology, University of Human Development, Sulaimaniyah 46001, Kurdistan Region, Iraq
**Corresponding Author Email: peshraw.abdalla@uoh.edu.iq*

ARTICLE DETAILS

Article History:

Received 15 September 2022
Revised 20 October 2022
Accepted 23 November 2022
Available online 30 November 2022

ABSTRACT

Skin cancer is a severe problem that is frequently disregarded. In circumstances of manual examination by a clinician, the human eye is occasionally unable to detect disorders precisely from imaging data. Deep learning techniques are increasingly being used nowadays to solve various problems in our daily lives. Therefore, deep neural network techniques are used to create an automated and computerized mechanism for detecting skin illnesses. To identify and diagnose skin illnesses over a range of criteria several neural network algorithms are evaluated and tested in the suggested model to see how well they perform. The networks are constructed to provide better outcomes using the CNN (Convolution neural network) and the Keras Sequential API architectures. The paper also compares the outcomes of the models using several metrics, such as accuracy, precision, f1 score, and recall. The transfer learning model involves seven models like DenseNet201, InseptionResnetV2, MobileNetV2, InceptionV3, ResNet50, DenseNet169, and VGG16. Among the employed models, the DenseNet169 model achieved the highest score of 87.58% in terms of accuracy; also, in terms of sensitivity and F1 score, DenseNet201 achieved the highest scores of 95.28% and 89.09%, respectively. On the other hand, VGG16 gained a score of 89.67% in terms of specificity, and DenseNet169 achieved the highest score of 90.64% in terms of precision.

KEYWORDS

CNN, Convolution neural network, Cancer detection, Cancer diagnosis, Deep learning, Machine learning, Neural networks, Skin cancer, Transfer learning.

1. INTRODUCTION

Due to its high prevalence, skin cancer is one of the world's most serious health issues relative to other cancer types. Skin malignancies are created by the growth of aberrant cells, which later, based on their type and intensity, may invade or spread to various parts of the body. The most delicate organ in our body is our skin because it is exposed to environmental contaminants the most. Consequently, skin cancer is the most prevalent and widespread among all cancer types. Nearly 46,000 new instances of skin cancer are recorded in the UK each year (Calabrò And Sternberg, 2006). One study found that the mortality rate was 90% lower when early-stage skin cancer was promptly identified (Khan et al., 2019). The biopsy process is typically used to detect skin cancer. A sample of a potential skin lesion must be removed for testing to establish whether it is cancerous.

However, it is a demanding, uncomfortable, and drawn-out process. Fortunately, with the aid of computer technologies, skin cancer signs can be identified more quickly, more easily, and more affordably (Dildar et al., 2021). These systems' main objective is to use high-quality clinical pictures with histological confirmation and machine learning algorithms to provide a preliminary evaluation of suspected skin diseases. Even though it cannot take the place of histology, which plays a critical role in tumor identification, the production of modern diagnostic tools can considerably aid in the early detection of malignant neoplasms in regions with a lack of practitioners and medical resources (Bhatt et al., 2022). Dermoscopy could be utilized to examine the hypodermis without requiring surgery, but for the best outcomes, a great deal of dermatology knowledge and experience is needed. Sadly, this method does not offer a firm melanoma diagnosis, particularly in the early stages. So, a tool for automatic diagnostics becomes a necessity.

Machine learning is commonly used in contemporary computer-based technology. It is a vast and quickly developing topic of AI(Artificial Intelligence) that gives computers the ability to autonomously learn and grow without needing to be specifically designed in various fields (Ismael et al., 2022). The technology was developed through the study of computational learning and pattern recognition theory, and it has recently been used in a wide variety of applications via several image-processing approaches (Ghafoor et al., 2021, Abdul et al., Rawf et al., 2022, Mohammed et al., 2020, Salih, 2015). Some other studies have focused on ways to provide better services for both hospitals and clients via cloud-based methods (Saeed and Ahmed, 2021; Abdalla and Varol, 2019). In this study, we have selected several state-of-the-art deep learning models for skin cancer detection and diagnosis via a transfer learning approach; for this purpose, we select the most well-known models. Next, the models

Quick Response Code	Access this article online	
	Website: www.actainformaticamalaysia.com	DOI: 10.26480/aim.01.2023.01.07

Cite the Article: Peshraw Ahmed Abdalla, Abdalbasit Mohammed Qadir, Omed Jamal Rashid, Sarkhel H. Taher Karim, Bashdar Abdalrahman Mohammed, Karzan Jaza Ghafoor (2023). Transfer Learning Models Comparison for Detecting and Diagnosing Skin Cancer. *Acta Informatica Malaysia, 7(1): 01-07.*

were trained with a specific skin cancer dataset, and finally, the results were compared in terms of accuracy, recall, F1-score, precision, and some other metrics.

2. Literature Review

A group reserchers offered skin identification, depending on the Maximum Entropy Threshold, extracting features by using the Gray Level Co-occurrence Matrix (GLCM) and classifying employing artificial neural networks (ANN) (Jaleel et al., 2013). For classification purposes, a back-propagation neural network (BPN) is employed. A group researchers employed segmentation as one of several clustering techniques in their research and the ABCD (Asymmetry Index Border Colour Index Diameter) method for extracting features (Krishna et al., 2016). According to, Amarathunga, to identify skin diseases, the forward chaining and rule-based approach were adopted by this system (Zia and Bukhari, 2022). The suggested system lets users diagnose children's skin conditions online and offer practical medical advice. The AdaBoost, BayesNet, MLP, and NaiveBayes were used, among other data mining classification methods, to predict and identify skin conditions.

This method is effective for three skin conditions (Melanoma, Eczema, and Impetigo). Rahi et al. suggested a CNN model with two different-strength Convolutional layers (Rahi et al., 2019). Between the input layer and the completely linked layer, these were merged with max-pooling layers in various configurations to create a total of 9 layers. To improve the outcomes, dropout layers have also been utilized. The collection consists of 2,967 pictures divided into benign and malignant categories. The 360 test photos and 1,440 benign and 1,197 malignant training images were selected (360 benign and 300 malignant). The proposed model produced results that were 84.76 percent accurate and 78.81 percent specific.

Daghrir et al. suggested a hybrid approach that combines KNN and SVM, two established machine learning algorithms, with a convolutional neural network (Daghrir et al., 2020). We received a dataset from the International Skin Imaging Collaboration (ISIC) database that included 640 pictures of lesions. One hundred twenty-eight of them were used for testing; then, training was done with the remaining 512. The input layer was followed by 3 convolutional layers, 3 max-pooling levels, 2 dropout layers, and a final fully connected layer for prediction, making up a total of 9 layers in the CNN architecture. The filters, morphological snake's method, Otsu method, and other preprocessing techniques were used. Before the majority vote (88.4% accuracy), the final classification was run on all three algorithms, with CNN providing the best individual accuracy at 85.5 percent and SVM coming in second at 71.8 percent.

3. Methods and Methodology

Numerous CNN models that have already been trained are used in this research. As convolutional layers make up the majority of CNN, models with varying numbers of layers, such as DenseNet201, InseptionResnetV2, InceptionV3, MobileNetV2, ResNet50, DenseNet169, and VGG16, have been developed. A single dataset is used to apply each model. These models are trained on the prepared dataset. Several different measures have been used to demonstrate the workings of these trained models.

3.1 Materials and Tools

Python is used for running these models as a programming language due to its popular libraries. To display statistical analysis and create visual graphs, libraries such as Matplotlib and Pandas are employed. With the NVidia K80 GPU, Kaggle has served as an IDE for these systems.

3.2 Dataset and Models

Without data, ML or AI models cannot be trained; therefore, a large amount of data is required to conduct deep learning experiments. A dataset from Kaggle called "'Skin Cancer' Malignant vs Benign" is used in this study. Overall, there are 3297 photos in this dataset (Fanconi C). The dataset is separated into two parts.: train part (2637 photos), which is applied when training models, and test part (660 photos); this is employed to assess the precision and other metrics of the trained models. There are 1497 total images in the malignant and 1800 images in the benign. The image sizes are all (600 × 450). All of the images are of a great calibre. Figure 1. displays some examples from the dataset for each class.

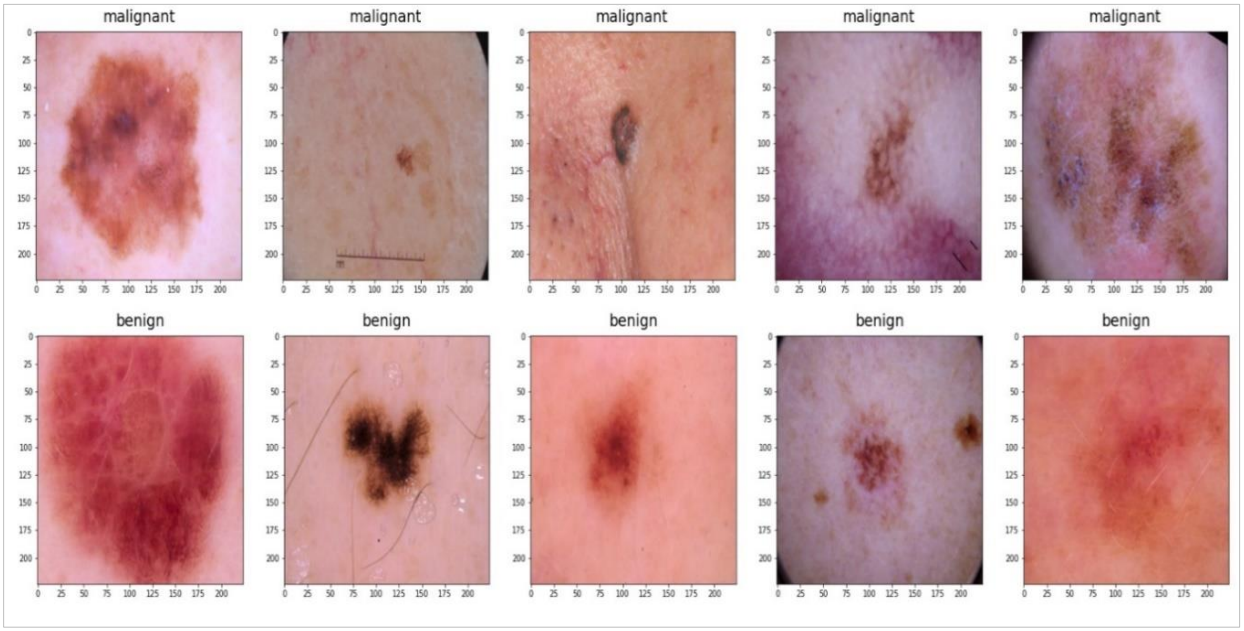

Figure 1: Some examples from the dataset for each class

We used a few methods for improving the quality of the photos in the preprocessing stage by changing the contrast and sharpness of the images with some noise removal methods in order to achieve higher results. Figure 2 demonstrates the system block diagram's operational process. This system starts by preparing data that is imported into it from Google Drive. Then, data is normalized using a variety of techniques, including image resizing, tagging, and null value reduction. Seven different neural network models are then trained, which are (DenseNet201, InseptionResnetV2, InceptionV3, MobileNetV2, ResNet50, DenseNet169, and VGG16). After using trained photos to train the system, it is adjusted to achieve the highest level of accuracy. Checking for over- and under-fitting in these models is one of the process' most crucial steps. Finally, test data is utilized to forecast and obtain an accurate output when the system is prepared for the final process. This working method is continued throughout the investigation.

3.3 Metrics

A common visual representation of the effectiveness of classification methods is a confusion matrix. The matrix (table) displays the proportion of correctly and wrongly identified instances in the test data in comparison to the actual results (target value). One benefit of using a confusion matrix (CM) as an approach for evaluation is that it enables more comprehensive analysis (such as when the model confuses two classes), as opposed to just looking at the proportion of examples that were correctly classified, which can produce false results if the dataset is unbalanced (Luque et al., 2019). For more explanation, we used several metrics such as specificity, sensitivity, negative predictive value, precision, false discovery rate, false positive rate, accuracy, false negative rate, f1 score, and matthews correlation coefficient.

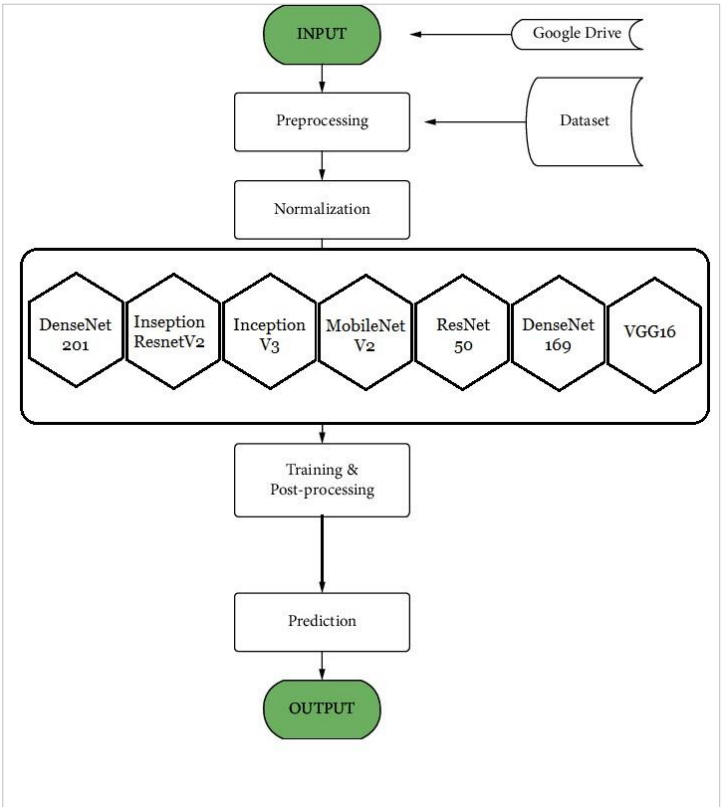

Figure 2: Block diagram for the system

- **Accuracy:** Through the use of CM parameters, accuracy can be determined. The entire quantity of accurate predictions is divided by the total quantity of forecasts in this case:

$$Accuracy = TP + TN / (TP + TN + FP + FN)$$

- **Precision:** Determines relevant instances from the obtained instances.

$$Precision = TP / (TP + FP)$$

- **Recall(sensitivity):** determines how many true positives there are overall, divided by the total number of true positives.

$$Recall = TP / (TP + FN)$$

- **F1 Score**: This strikes a balance between recall and precision. This is a more accurate way to assess test accuracy.

$$F1\ Score = 2 * (Precision * Recall) / (Precision + Recall)$$

- **False Discovery Rate**

$$FDR = FP / (FP + TP)$$

- **False Positive Rate**

$$FPR = FP / (FP + TN)$$

- **False Negative Rate**

$$FNR = FN/(FN + TP)$$

- **Negative Predictive Value**

$$NPV = TN / (TN + FN)$$

- **Matthews Correlation Coefficient**

$$TP * TN - FP * FN / sqrt((TP + FP) * (TP + FN) * (TN + FP) * (TN + FN))$$

3.4 Network Architecture

3.4.1 Inception V3

The third version of the Deep Learning Convolutional Architectures, Inception V3, has been suggested by Google. The ImageNet dataset, which was itself trained on over one million photos, provided the model with 1000 classes for use in training. The input image needs to be 299 by 299 pixels in size in order to use the ImageNet pre-trained weight of the Inception V3 network.

3.4.2 VGG16 Model

Convolutional neural network (CNN) architecture VGG16 won the 2014 ILSVRC (Imagenet) contest. It is well known for being among the most cutting-edge vision model architectures ever created. Throughout the architecture, the placement of the convolutional and max-pool layers is the same. Two completely interconnected layers and a softmax for the result are used to close it (Pandiyan et al., 2019). The number 16 in VGG16 indicates that there are 16 layers with various values. This system contains an estimated 138 million elements.

3.4.3 ResNet50

A popular neural network model utilized as a key component for numerous computer vision tasks is called Residual Network (ResNet). The 2015 ImageNet competition was won by this ResNet model. The input image size for the 50-layer network is 224 by 224 pixels (He et al., 2016).

3.4.4 MobileNetV2

The 53 layers of MobileNet-v2 are convolutional neural networks. A pre-trained network using more than a million images in the ImageNet database is available for loading. The pre-trained network is capable of classifying photos into 1000 different object categories. This has led to network learning detailing a range of image representations with features. The network's picture input is 224 × 224 pixels. (Patel and Chaware, 2020).

3.4.5 DenseNet201 and 169

A convolutional neural network of 201 and 169 layers deep is called DenseNet201and DenseNet169. A pre-trained version of the network that has been trained on more than one million photographs is available in the ImageNet database. One thousand different object categories can be identified in pictures using the pre-trained network. As a result, For a range of photos, the network has collected extensive feature representations. The network can accept images up to 224 by 224 pixels (Wang et al., 2020).

3.4.6 InceptionResNetV2

Using more than a million photos from the ImageNet collection, the convolutional neural network Inception-ResNet-v2 was trained. The 164-

layer deep network is capable of classifying photos into 1000 different object categories. Consequently, For many different photos, the network has gathered rich feature representations. The network accepts photos with a resolution of 299 by 299 (Mannepalli et al., 2022).

4. Results and Discussion

4.1 DenseNet201

The DenseNet201 model's classification performance is shown in this section. Since the input for this model must be in the 224 by 224 format, the input photos were downsized to that size. The model's confusion matrix is displayed in Table 1.

4.2 InceptionResNetV2

The InceptionResNetV2 model's classification performance is shown in this section. Since the input for this model must be in the 229 by 229 format, the input photos were downsized to that size. The model's confusion matrix is displayed in Table 2.

4.3 InceptionV3

The InceptionV3 model's classification performance is shown in this section. Since the input for this model must be in the 229 by 229 format, the input photos were downsized to that size. Figure 9 displays the loss and accuracy for the test and validation phases of the model. The model's confusion matrix is displayed in Table 3.

4.4 MobileNetV2

The MobileNetV2 model's classification performance is shown in this section. Since the input for this model must be in the 224 by 224 format, the input photos were downsized to that size. Figure 11 displays the loss and accuracy for the test and validation phases of the model. The model's confusion matrix is displayed in Table 4.

4.5 ResNet50

The ResNet50 model's classification performance is shown in this section. Since the input for this model must be in the 224 by 224 format, the input photos were downsized to that size. Figure 13 displays the loss and accuracy for the test and validation phases of the model. The model's confusion matrix is displayed in Table 5.

4.6 DenseNet169

The DenseNet169 model's classification performance is shown in this section. Since the input for this model must be in the 224 by 224 format, the input photos were downsized to that size. Figure 15 displays the loss and accuracy for the test and validation phases of the model. The model's confusion matrix is displayed in Table 6. This model's categorization report is included in Table 12 for each class. Figure 16 shows the average metrics the model attained.

4.7 VGG16

The VGG16 model's classification performance is shown in this section. Since the input for this model must be in the 224 by 224 format, the input photos were downsized to that size. Figure 17 displays the loss and accuracy for the test and validation phases of the model. The model's confusion matrix is displayed in Table 7.

Table 1: ResNet201 Confusion Matrix

		Benign	Malignant
True Classes	Benign	**343**	17
	Malignant	67	**233**
	Predicted Classes		

Table 2: InceptionResNetV2 Confusion Matrix

		Benign	Malignant
True Classes	Benign	**290**	70
	Malignant	41	**259**
	Predicted Classes		

Table 3: InceptionV3 Confusion Matrix

		Benign	Malignant
True Classes	Benign	**322**	38
	Malignant	86	**214**
	Predicted Classes		

Table 4: MobileNetV2 Confusion Matrix

		Benign	Malignant
True Classes	Benign	**313**	47
	Malignant	54	**246**
	Predicted Classes		

Table 5: ResNet50 Confusion Matrix

		Benign	Malignant
True Classes	Benign	**341**	19
	Malignant	177	**123**
	Predicted Classes		

Table 6: DenseNet169 Confusion Matrix

		Benign	Malignant
True Classes	Benign	**310**	50
	Malignant	32	**268**
	Predicted Classes		

Table 7: VGG16 Confusion Matrix			
		Benign	Malignant
True Classes	Benign	**283**	77
	Malignant	31	**269**
	Predicted Classes		

5. Comparison of Model Performances

Figure 3. explains accuracy and loss for the models in both the test and validation phases. Table 8 eplians classification report per each class. Table 9 gives us a comprehensive view of all seven convolutional neural network systems that were used in this work. Figure 4 explains the overall outcomes visually.

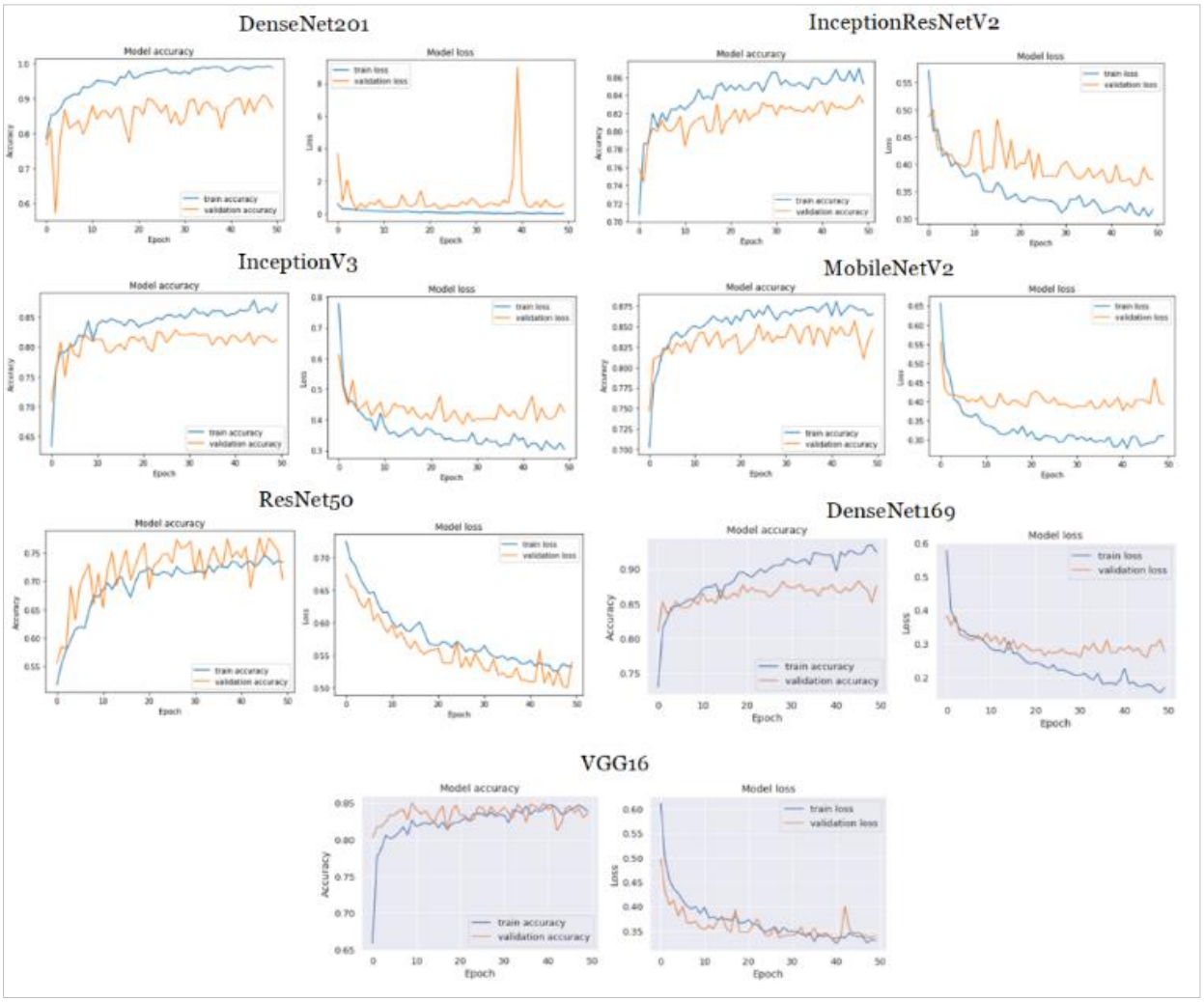

Figure 3: Accuracy and loss for the models in both the test and validation phases

Table 8: Classification Report Per Each Class							
Model	Class	Tets images	Classified images	Accuracy	Precision	Recall	F1 Score
ResNet201	benign	360	410	83.65%	0.84	0.95	0.89
	malignant	300	250	93.20%	0.93	0.78	0.85
InceptionResNetV2	benign	360	331	87.08%	0.88	0.81	0.84
	malignant	300	329	78.72%	0.79	0.86	0.82
InceptionV3	benign	360	408	78.92%	0.79	0.89	0.84
	malignant	300	252	84.92%	0.85	0.71	0.78
MobileNetV2	benign	360	367	85.28%	0.85	0.87	0.86
	malignant	300	293	83.95%	0.84	0.82	0.83
ResNet50	benign	360	518	65.83%	0.66	0.95	0.78
	malignant	300	142	86.61%	0.87	0.41	0.56
DenseNet169	benign	360	342	90.64%	0.91	0.86	0.88
	malignant	300	318	84.27%	0.84	0.89	0.87
VGG16	benign	360	314	90.12%	0.90	0.79	0.84
	malignant	300	346	87.74%	0.78	0.90	0.83

Table 9: A Comparative Analysis of The Models

Measure	DenseNet201	InceptionResNetV2	InceptionV3	MobileNetV2	ResNet50	DenseNet169	VGG16
Sensitivity	**0.9528**	0.8633	0.8944	0.8694	0.9472	0.8611	0.7861
Specificity	0.7767	0.8761	0.7133	0.8200	0.4100	0.8933	**0.8967**
Precision	0.8366	0.7872	0.7892	0.8529	0.6583	**0.9064**	0.9013
Negative Predictive Value	0.9320	0.1367	0.8492	0.8396	0.8662	0.8428	0.7775
False Positive Rate	0.2233	0.1239	0.2867	0.1800	0.5900	0.1067	0.1033
False Discovery Rate	0.1634	0.1944	0.2108	0.1471	0.3417	0.0936	0.0987
False Negative Rate	0.0472	0.8318	0.1056	0.1306	0.0528	0.1389	0.2139
Accuracy	0.8727	0.8394	0.8121	0.8470	0.7030	**0.8758**	0.8364
F1 Score	**0.8909**	0.6661	0.8385	0.8611	0.7768	0.8832	0.8398
Matthews Correlation Coefficient	0.7488	0.8633	0.6229	0.6909	0.4329	0.7518	0.6808

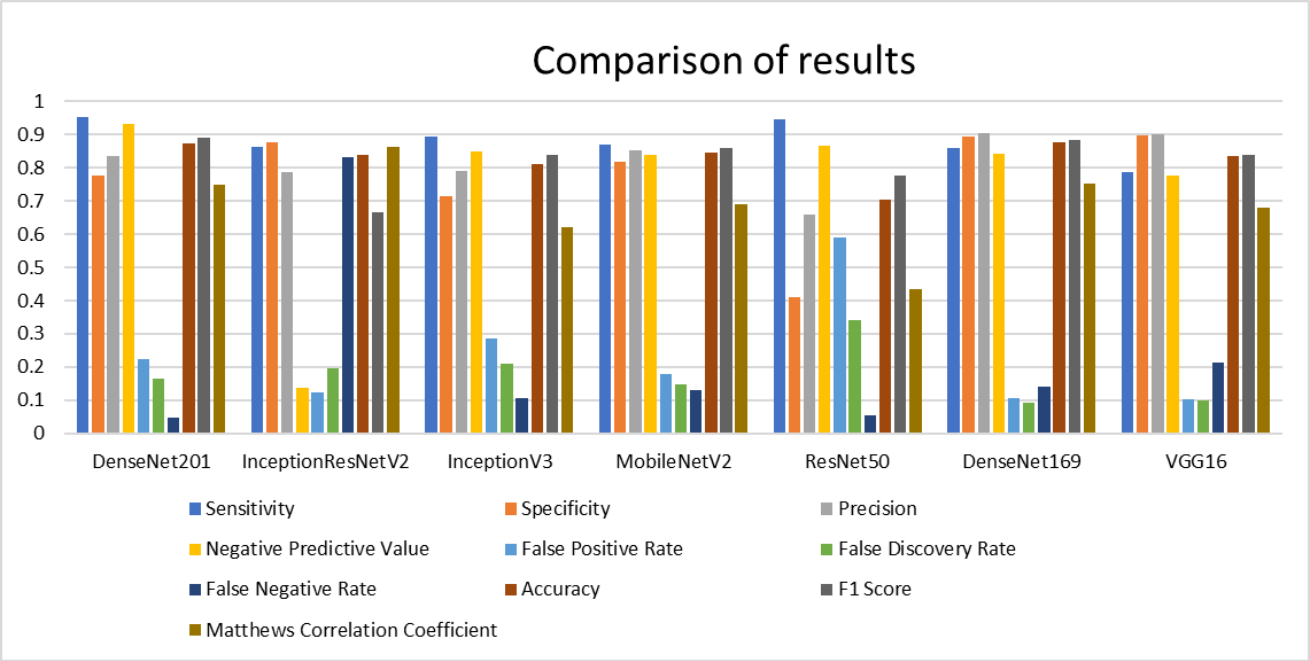

Figure 4: Overall outcomes achieved by the models

6. Conclusion

There are many terrible diseases in the modern world, including skin cancer. To prevent this type of cancer from happening, an early diagnosis is the best strategy to take. Medical knowledge has evolved in the modern world. In the past, skin cancer had to be identified manually, which was time-consuming and expensive. However, advances in deep learning in medicine have made it easier. Deep learning techniques, especially CNNs, can detect skin cancer quickly and cheaply. This study suggests using CNN to detect skin cancer as a consequence. Several different convolutional neural network models were employed in this study, such as (DenseNet201, InseptionResnetV2, InceptionV3, MobileNetV2, ResNet50, DenseNet169, and VGG16).

We tested the models using a number of metrics after applying several convolutional models to the dataset. The DenseNet169 model achieved the highest score of 87.58% in terms of accuracy, while in terms of sensitivity and f1 score, DenseNet201 achieved the highest score of 95.28% and 89.09%, respectively; on the other hand, VGG16 gained a score of 89.67% in terms of specificity, the highest score of precision 90.64% is achieved by DenseNet169. This method was developed to look for possible skin cancer. Doctors will be able to quickly and easily detect skin cancer at an early stage. Our long-term goal is to apply our skin cancer detection models in real-world settings so that those with limited access to medical care can benefit from our work.

References

Abdalla, P.A., and Varol, A., 2019. Advantages to Disadvantages of Cloud Computing for Small-Sized Business. 7th International Symposium on Digital Forensics and Security (ISDFS). IEEE.

Abdul, Z.K., Al-Talabani, A., Abdulrahman, A.O.J.S., 2016. Vibration A new feature extraction technique based on 1D local binary pattern for gear fault detection.

Bhatt, H., Shah, V., Shah, K., Shah, R., and Shah, M.J.I.M., 2022. State-of-the-art machine learning techniques for melanoma skin cancer detection and classification: a comprehensive review.

Calabrò, F., and Sternberg, C.N., 2006. Cancer and its Management. Wiley Online Library.

Daghrir, J., Tlig, L., Bouchouicha, M., and Sayadi, M., 2020. Melanoma skin cancer detection using deep learning and classical machine learning techniques: A hybrid approach. 2020 5th international conference on advanced technologies for signal and image processing (ATSIP), IEEE, Pp. 1-5.

Dildar, M., Akram, S., Irfan, M., Khan, H.U., Ramzan, M., Mahmood, A.R., Alsaiari, S.A., Saeed, A.H.M., Alraddadi, M.O., Mahnashi, M.H., 2021. Skin cancer detection: a review using deep learning techniques, 18, Pp. 5479.

Fanconi C. Skin cancer: malignant vs. Benign," processed skin cancer pictures of the ISIC archive Kaggle dataset [Online]. Available: https://www.kaggle.com/fanconic/skin-cancer-malignant-vs-benign [Accessed].

Ghafoor, K.J., Rawf, K.M.H., Abdulrahman, A.O., Taher, S.H., 2021. Kurdish dialect recognition using 1D CNN., 9, Pp. 10-14.

He, K., Zhang, X., Ren, S., and Sun, J., Deep residual learning for image recognition. Proceedings of the IEEE conference on computer vision and pattern recognition, Pp. 770-778.

Ismael, Y.S., Shakor, M.Y., Abdalla, P.A., 2022. Deep Learning Based Real-Time Face Recognition System. NeuroQuantology, 20, Pp. 355-7366.

Jaleel, J.A., Salim, S., Aswin, R., 2013. Computer aided detection of skin cancer. International Conference on Circuits. Power and Computing Technologies (ICCPCT), IEEE, Pp. 1137-1142.

Khan, M.Q., Hussain, A., Rehman, S.U., Khan, U., Maqsood, M., Mehmood, K., Khan, M.A., 2019. Classification of melanoma and nevus in digital images for diagnosis of skin cancer, 7, Pp. 90132-90144.

Krishna, M.C., Ranganayakulu, S., Venkatesan, D.P., 2016. Skin cancer detection and feature extraction through clustering technique, Pp. 4.

Luque, A., Carrasco, A., Martín, A., De Las Heras, A.J.P.R., 2019. The impact of class imbalance in classification performance metrics based on the binary confusion matrix. 91, Pp. 216-231.

Mannepalli, D.P., Namdeo, V.J., 2022. An effective detection of COVID-19 using adaptive dual-stage horse herd bidirectional long short-term memory framework.

Mohammed, A.A., Salih, D.A., Saeed, A.M., 2020. An imperceptible semi-blind image watermarking scheme in DWT-SVD domain using a zigzag embedding technique, 79, Pp. 32095-32118.

Pandiyan, V., Murugan, P., Tjahjowidodo, T., Caesarendra, W., Manyar, O.M., Then, D.J.H., 2019. In-process virtual verification of weld seam removal in robotic abrasive belt grinding process using deep learning, 57, Pp. 477-487.

Patel, R., and Chaware, A., 2020. Transfer learning with fine-tuned MobileNetV2 for diabetic retinopathy. 2020 international conference for emerging technology (INCET). IEEE, Pp. 1-4.

Rahi, M.M.I., Khan, F.T., Mahtab, M.T., Ullah, A.A., Alam, M.G.R., Alam, M.A., 2019. Detection of skin cancer using deep neural networks. Asia-Pacific Conference on Computer Science and Data Engineering (CSDE), Pp. 1-7.

Rawf, K.H., Abdulrahman, A., Mohammed, A., 2022. Effective Kurdish Sign Language Detection and Classification Using Convolutional Neural Networks.

Saeed, M.H., and Ahmed, B.T., 2021. Web-Based Dental Patient Education And Management Application. Acta Informatica Malaysia, 5, Pp. 12-15.

Salih, D., 2015. School Of Computer Science, University Of Birmingham, Birmingham. Natural User Interfaces, Pp. 369-375.

Wang, S.H., Zhang, Y.D., 2020. DenseNet-201-based deep neural network with composite learning factor and precomputation for multiple sclerosis classification. 16, Pp. 1-19.

Zia, G., and Bukhari, Z., 2022. A healthcare model to predict skin cancer using deep extreme machine learning. 1, Pp. 23-30.